Night sky at the Indian Astronomical Observatory during 2000–2008

C. S. Stalin*, M. Hegde, D. K. Sahu, P. S. Parihar, G. C. Anupama,
B. C. Bhatt and T. P. Prabhu
Indian Institute of Astrophysics, Bangalore 560 034, India

Abstract. This paper presents an analysis of the optical night sky brightness and extinction coefficient measurements in $UBVRI$ at the Indian Astronomical Observatory (IAO), Hanle, during the period $2000-2008$. They are obtained from an analysis of CCD images acquired at the 2 m Himalayan Chandra Telescope (HCT) at IAO. Night sky brightness was estimated using 210 HFOSC images obtained on 47 nights and covering the declining phase of solar activity cycle-23. The zenith corrected values of the moonless night sky brightness in mag arcsec^{-2} are 22.14 ± 0.32 (U), 22.42 ± 0.30 (B), 21.28 ± 0.20 (V), 20.54 ± 0.37 (R) and 18.86 ± 0.35 (I) band. This shows that IAO is a dark site for optical observations. No clear dependency of sky brightness with solar activity (implied by the 10.7 cm solar flux) is found. Extinction values at IAO are derived from an analysis of 1325 images over 58 nights. They are found to be 0.36 ± 0.07 in U-band, 0.21 ± 0.04 in B-band, 0.12 ± 0.04 in V-band, 0.09 ± 0.04 in R-band and 0.05 ± 0.03 in I-band. On an average, extinction during the summer months is slightly larger than that during the winter months. This might be due to an increase of dust in the atmosphere during the summer months. No clear evidence for a correlation between extinction in all bands and the average night time wind speed is found. Also, presented here, is the low resolution moonless optical night sky spectrum for IAO covering the wavelength range $3000 - 9300$ Å. Features from O, OH, N and Na are seen in the spectra. Hanle, thus has the required characteristics of a good astronomical site in terms of night sky brightness and extinction, and could be a natural candidate site for any future large aperture Indian optical-infrared telescope(s).

Keywords : atmospheric effects, site testing

*e-mail:stalin@iiap.res.in

1.   Introduction

A good astronomical site is characterised by various atmospheric conditions (which includes atmospheric transparency, seeing, meteorological parameters such as wind, snowfall, surface temperature, rainfall etc. and sky brightness) and geographical conditions (such as local topography, seismicity, source availability i.e, latitude etc.). Sites having minimum cloud coverage, very low frequency of snowfall/rainfall, low relative humidity, low nocturnal temperature variation, high atmospheric transparency and low night sky brightness are good for ground-based optical and infrared observations. Two main characteristics of the night sky are the night sky brightness and atmospheric extinction.

Even in the absence of artificial light, the moonless night sky is not dark. This is because the atmosphere scatters into the sky, light emitted by the following processes (cf. Krisciunas 1997), (i) zodiacal light (caused by sunlight scattered off interplanetary dust), (ii) faint unresolved stars and diffuse galactic light due to atomic processes within our galaxy, (iii) diffuse extragalactic light (due to distant, faint unresolved galaxies) and (iv) airglow and aurorae (produced by photochemical reactions in the Earth's upper atmosphere). Of these, (i)−(iii) are extraterrestrial in origin and thus independent of the site, whereas (iv) depends on the site and time of observation. These are the natural processes which produce the night sky brightness in any astronomical site. In addition to the above, night sky can be affected by light pollution due to scattering of street lights in the Earth's lower atmosphere. Although we do not have control on any of the natural sources causing the brightness of the night sky, we do have control on the brightness caused by artificial lights scattered onto the sky. It is thus possible to maintain the night sky brightness at any observatory site to its natural level by minimising light pollution in the immediate vicinity of the observatory.

Apart from the natural and artificial sources affecting the night sky, the light coming from any celestial source being observed suffers from scattering by air molecules and aerosols as well as absorption by water vapour and ozone while passing through the Earth's atmosphere. This leads to attenuation of their light and is referred to as the atmospheric extinction. This depends on the constituents of the atmosphere, the wavelength of the incoming light, and the altitude of the site. Precise knowledge of the extinction coefficient of each site is essential to compare observations of the same object taken from different locations of the globe. A good astronomical site needs low extinction values. Apart from low extinction, its stability during the night is also equally important.

In this article, we present, the moonless night sky brightness and atmospheric extinction in $UBVRI$ passbands at IAO, Hanle. IAO is located at the Himalayan range in Northern India (longitude = $78°57'51.2''$ E, latitude = $32°46'46.5''$ N and altitude = 4467 m) and run by the Indian Institute of Astrophysics, Bangalore. This is a thinly populated, cold and dry desert region. The sky at IAO is thus not much affected by dust and light pollution due to human activities. The 2 m Himalayan Chandra Telescope (HCT) is operational at IAO since May 2003. The data used in this study for night sky

brightness span the period 2003−2008 which correspond to a major part of the declining phase of solar activity (which could affect night sky brightness) cycle-23, while the data for extinction estimates span the period 2000−2008. Preliminary estimates of the night sky brightness and extinction at IAO have been reported by Parihar et al. (2003) and an analysis of the meteorological parameters at IAO is presented in Stalin et al. (2008). The structure of this paper is as follows. Section 2 describes the data set used in this study, Section 3 presents the analysis of extinction and Section 4 presents an analysis of night sky brightness. A spectrum of the night sky at IAO is presented in Section 5 and the results are summarized in the final section.

2.   Data

Data were not obtained specifically for studying the night sky at IAO. Therefore, archives at IAO were searched for a data set which is as homogeneous as possible. Multiband imaging data from the supernova monitoring program of IAO were thus collected from the archives spanning the years 2003−2008. They were from science observations carried out using HFOSC at the 2 m HCT. The CCD used in these observations was a 2k × 4k, with a pixel scale of $0.296''$/pix giving a sky coverage of 10×10 arcmin^2. A total of 210 images obtained over 47 nights were extracted from the IAO archives and used to estimate the night sky brightness. Photometric standard fields (Landolt 1992) observed over several nights during 2000−2008 were used to estimate the site extinction. A 1k × 1k CCD system was in use during 2000−2002, while the HFOSC was used since 2003 February. The data used for extinction estimates thus comprise of a total of 1325 image frames in the $UBVRI$ bands obtained over 58 nights, covering an airmass range of 1.01 − 2.40. Pre-processing of all the photometric data as well as photometry have been done using IRAF[1].

The night sky spectrum at IAO has been extracted from the spectroscopic data of supernova SN 2004et obtained on 2004 October 16. The spectra were obtained with a $11'$ long and $1.92''$ wide slit and two grisms; grism 7 and grism 8 covering the wavelength range from 3500−7000 Å and 5200−9200 Å respectively. The spectral resolution is 8 Å. Spectroscopic data too, was bias subtracted, flux and wavelength calibrated using standard IRAF procedures.

3.   Extinction

The Bouguer's linear formula for atmospheric extinction is

$$m(\lambda, z) = m_o(\lambda) + 1.086 k_\lambda secz \tag{1}$$

---

[1]IRAF is distributed by the National Optical Astronomy Observatories, which is operated by the Association of Universities for Research in Astronomy Inc. under contract to the National Science Foundation

where $m(\lambda, z)$ is the observed magnitude, $m_o(\lambda)$ is the magnitude above the Earth's atmosphere, k_λ is the extinction and secz is the airmass at zenith distance z.

The three sources of extinction in the Earth's atmosphere that are important for ground based astronomical photometry are (Hayes & Latham 1975)

1. A_{aer} = Aerosol scattering

2. A_{Ray} = Rayleigh scattering by molecules

3. A_{oz} = molecular absorption mainly by ozone

The contribution of each of these parameters to extinction depends on wavelength, whereas, Rayleigh and Aerosol scattering, apart from wavelength, depend also on height and atmospheric conditions at the site.

According to Hayes & Latham (1975), Rayleigh scattering by air molecules at an altitude h is given by

$$A_{Ray}(\lambda, h) = 9.4977 \times 10^{-3} \left(\frac{1}{\lambda}\right)^4 C^2 \times exp\left(\frac{-h}{7.996}\right) \tag{2}$$

where $C = 0.23465 + \frac{1.076 \times 10^2}{146 - (1/\lambda)^2} + \frac{0.93161}{41 - (1/\lambda)^2}$

Here, λ is the wavelength in microns and h is the altitude in km. Eq.2 assumes an atmospheric pressure of 760 torr at $h = 0$ and a scale height of 7.996 km. The largest uncertainty here is due to the deviation of local atmospheric pressure from the assumed standard condition.

Molecular absorption by ozone and water vapour too contribute to the total extinction at any site. Ozone is concentrated at altitudes between 10 and 35 km and hence its contribution to the extinction does not depend on the altitude of the observatory. However, it is a function of wavelength and occurs in selective bands centered at $\lambda\lambda$ 3300 and 5750 Å (Gutierrez-Moreno et al. 1982). On the other hand, extinction due to water vapour is difficult to estimate, because the amount of water vapour above a site is variable. This is however, weak and centered only around a few select bands with neglible contribution to broad band. The extinction due to ozone is (cf. Bessel 1990; Kumar et al. 2000)

$$A_{oz} = 0.2775 C_{oz}(\lambda) \tag{3}$$

where $C_{oz}(\lambda)$ is the ozone absorption coefficient and is given as

$$C_{oz}(\lambda) = 3025 exp\left(-131(\lambda - 0.26)\right) + 0.1375 exp\left(-188(\lambda - 0.59)^2\right). \tag{4}$$

Extinction due to aerosol scattering is highly variable. This is due to particulates including mineral dust, salt particles and man-made pollutants and is expressed as

$$A_{aer}(\lambda, h) = A_o \lambda^{-\alpha} exp(-h/H) \tag{5}$$

where H is the density scale height for aerosols and A_o is the total optical thickness of atmospheric aerosols for $\lambda = 1\ \mu m$, which depends on the total content of particles and on their efficiency for scattering and absorption and is taken to be 0.087 (Mohan et al. 1999; Bessel 1990). α is a parameter which depends on the size of the aerosol grains. Following Hayes & Latham (1975) a value of $H = 1.5$ km and $\alpha = 0.8$ is considered in this work. The largest uncertainty in A_{aer} from Eq. 5, is due to the incomplete knowledge of the nature of aerosols at the location of IAO.

The total extinction at any given wavelength is therefore a linear combination of these three contributions and is given as

$$A_\lambda = A_{aer}(\lambda, h) + A_{Ray}(\lambda, h) + A_{oz}(\lambda). \tag{6}$$

The extinction coefficients in different filters were determined using Eq. 1 from HFOSC images. The observed values at U, B, V, R and I filters and the theoretical values calculated at their central wavelengths are given in Table 1. The observed values of extinction coefficients have a mean value of 0.36 ± 0.07, 0.21 ± 0.04, 0.12 ± 0.04, 0.09 ± 0.04 and 0.05 ± 0.03 in $UBVRI$ bands respectively. A histogram of the measured extinction coefficients is shown in Fig. 1. The monthly variation of extinction determined for the period $2000-2008$ is shown in Fig. 2. From Fig. 2 it is seen that the extinction in summer months is larger than during the winter months. Here, summer months refer to the period between May$-$September and winter months refer to the period between October$-$April. The variation of the measured extinction coefficients with the average night time wind speed is shown in Fig. 3 for all the bands. From Fig. 3, there is a hint for a correlation between the extinction coefficient and the wind speed. But, non-inclusion of one high extinction value at high wind speed in each band removes the correlation (linear correlation coefficient R < 0.5) and the linear fit shown in Fig. 3 almost becomes horizontal. Thus, from the present data set, there is no clear evidence of a correlation between the extinction coefficient and the average night time wind speed. Further data are needed to check for the presence or absence of this correlation. A statistical summary of the measured extinction data is given in Table 2. The yearly averages of extinction coefficient in several bands are given in Table 3. As evident from Table 3, we find no clear evolution of extinction over the years $2000-2008$.

3.1 Nature of aerosols at IAO

Aerosol extinction properties can be studied from the observed total extinction. The observed values of mean extinction were analysed to study the nature of aerosols at IAO. It has been noted by Hayes & Latham (1975) that the extinction due to Rayleigh and ozone can be calculated theoretically with an accuracy of the order of ± 0.01 mag/airmass for wavelengths between $3300 - 10800$ Å, using Eqs. 2 and 3. Therefore, from the total measured extinction, theoretically calculated values of extinction due to Rayleigh

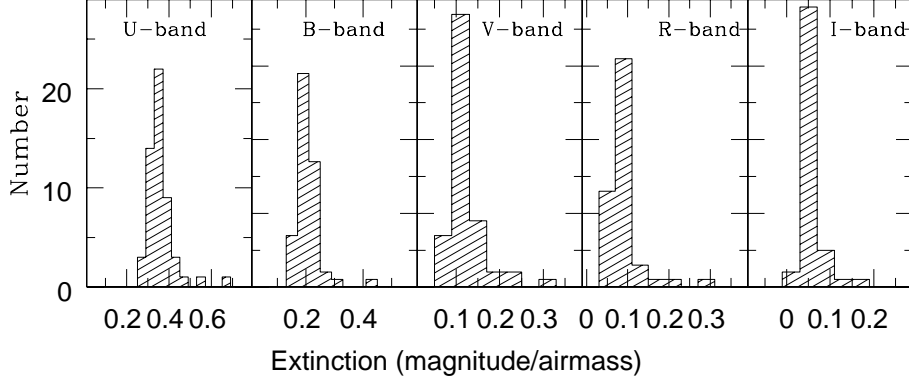**Figure 1.** Distribution of the measured extinction coefficients in magnitude/airmass at IAO in $UBVRI$ bands

Table 1. The calculated and measured values of the extinction coefficients in mag/airmass at Hanle.

Filter	$\lambda_{0\overset{\circ}{A}}$	k_{Ray}	k_{aer}	k_{oz}	k_{sum}	Observed
U	3650	0.3307	0.0099	0.0008	0.3414	0.36 ± 0.07
B	4400	0.1522	0.0085	0.0005	0.1612	0.21 ± 0.04
V	5500	0.0610	0.0071	0.0262	0.0943	0.12 ± 0.04
R	7000	0.0229	0.0059	0.0036	0.0324	0.09 ± 0.04
I	8800	0.0091	0.0049	0.0000	0.0140	0.05 ± 0.03

scattering and ozone were subtracted to get the observed values of extinction due to aerosols. Thus the extinction due to aerosols at IAO is estimated as follows

$$A_{aer}(\lambda) = <A> - A_{Ray}(\lambda) - A_{oz}(\lambda). \tag{7}$$

The deduced values of aerosols using Eq. 7 could well be represented as

$$A_{aer} = \beta\lambda^{-\alpha} \tag{8}$$

α and β in Eq. 8, were then determined by linear fits on the log-log plots of the deduced aerosol extinction and wavelength. We find a mean value of $\alpha = 0.84 \pm 0.23$ and $\beta = 0.07 \pm 0.04$ from analysis of 14 nights for which a linear fitting was possible. The mean value of α found here is similar to that found for many observatories (Hayes & Latham 1975). A comparison of the extinction at Hanle with that of other sites is given in Table 4. From Table 4 it is seen that the extinction at IAO is similar to that of the best astronomical sites.
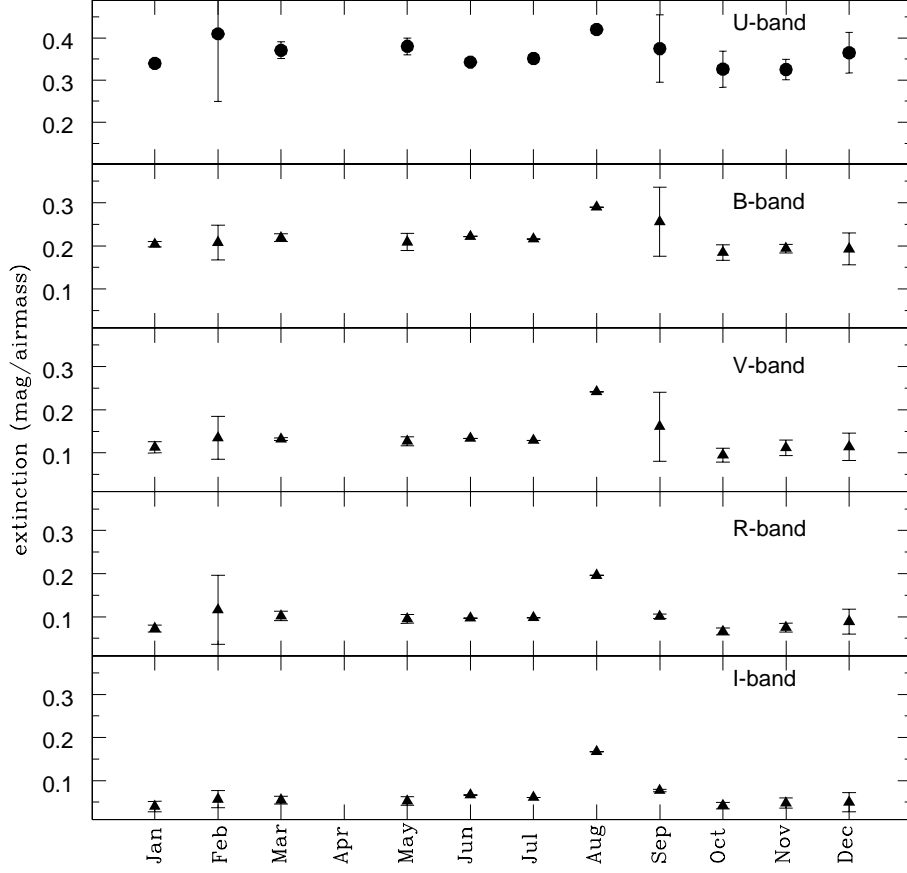
Figure 2. Monthly variation of extinction at IAO during the period 2003−2007. The error bars when not visible are less than the size of symbols. These error bars represent the scatter in the values, the accuracy of individual measurements being much smaller.

4. Sky brightness

The night sky brightness is estimated following the relation given by Krisciunas et al. (2007):

$$S = -2.5log\left(\frac{C_{sky}}{C_*}\right) + 2.5log\left(\frac{E_{sky}}{E_*}\right) + K_\lambda X_* + M_* \qquad (9)$$

where S is the brightness of the sky in magnitudes, C_* is the total counts above sky within the aperture of the standard star of magnitude M_* with an exposure time E_*, C_{sky} is the mean sky counts times the area of the aperture with exposure E_{sky}. X_* is the airmass and k_λ is the atmospheric extinction corresponding to the filter used. The sky brightness
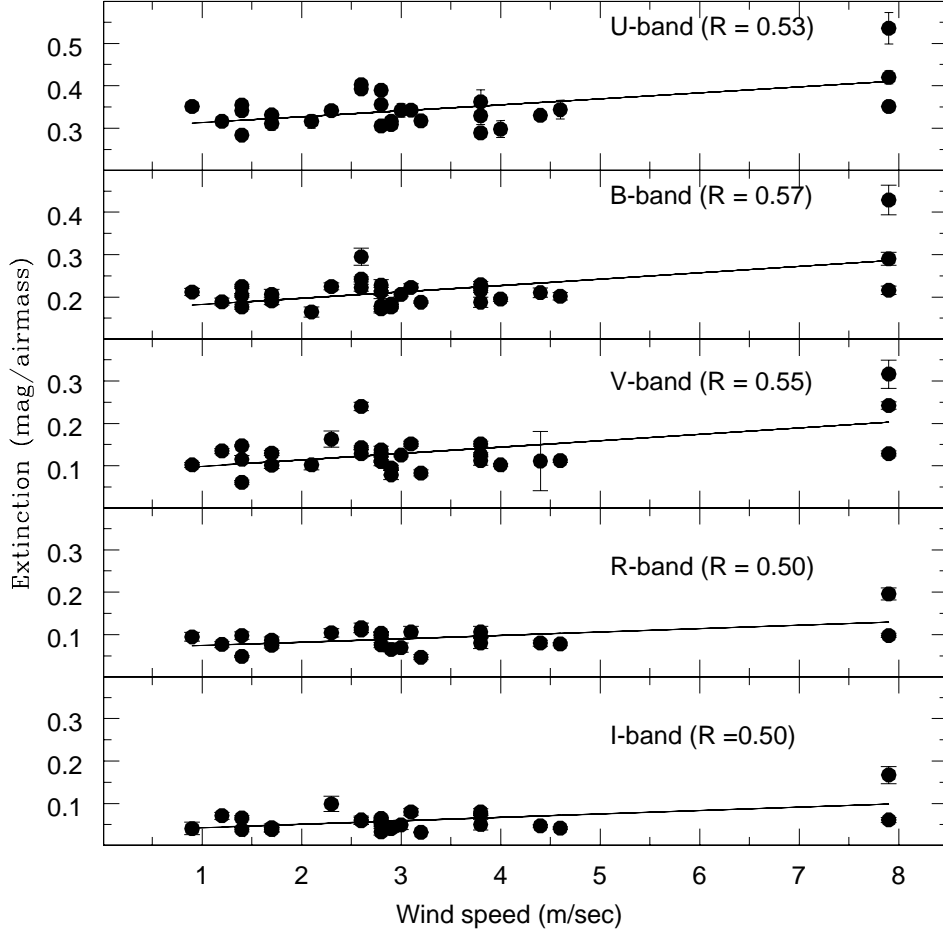
Figure 3. Variation of extinction in $UBVRI$ passbands with the average night time wind speed. The linear correlation coefficient in each band is given in the respective panel. The error bars when not visible are smaller than the symbol size. The solid line is the unweighted linear least squares fit to the data.

in magnitude per square arcsec, I(μ) is then

$$I(\mu) = S + 2.5 logA \qquad (10)$$

Here, A is the area of the aperture in square arcseconds estimated from the plate scale of the CCD. It is known that the sky becomes brighter at larger airmass. This is due to the natural effect of airglow which is brighter at low elevations. Light pollution also makes the sky brighter at low elevations. On the other hand, the contribution of extra-terrestrial component to sky brightness is independent of zenith distance. The images

Table 2. Extinction coefficients in mag/airmass at Hanle for the whole period as well as for summer and winter months.

Filter	Total		Summer		Winter	
	Nights	Mean	Nights	Mean	Nights	Mean
U	54	0.36 ± 0.07	10	0.38 ± 0.06	44	0.35 ± 0.07
B	57	0.21 ± 0.04	11	0.24 ± 0.07	46	0.20 ± 0.03
V	58	0.12 ± 0.04	11	0.15 ± 0.06	47	0.12 ± 0.03
R	50	0.09 ± 0.04	08	0.11 ± 0.03	42	0.09 ± 0.04
I	47	0.05 ± 0.03	08	0.08 ± 0.04	39	0.05 ± 0.02

Table 3. Average yearly Extinction in mag/airmass at IAO.

Year	U	B	V	R	I
2000	0.38 ± 0.04	0.19 ± 0.03	0.12 ± 0.02	0.09 ± 0.02	0.05 ± 0.01
2002	0.35 ± 0.04	0.21 ± 0.03	0.12 ± 0.04	0.09 ± 0.04	0.05 ± 0.03
2003	0.38 ± 0.08	0.25 ± 0.10	0.15 ± 0.09	0.07 ± 0.01	0.03 ± 0.01
2004	0.34 ± 0.06	0.21 ± 0.06	0.13 ± 0.06	0.09 ± 0.04	0.06 ± 0.04
2005	0.37 ± 0.10	0.22 ± 0.03	0.14 ± 0.04	0.11 ± 0.06	0.06 ± 0.02
2006	0.34 ± 0.04	0.21 ± 0.01	0.12 ± 0.01	0.09 ± 0.02	0.06 ± 0.01
2007			0.09 ± 0.00	0.06 ± 0.00	0.03 ± 0.00
2008		0.19 ± 0.04	0.10 ± 0.05	0.07 ± 0.02	0.06 ± 0.03

Table 4. Comparison of extinction in mag/airmass at various sites.

Site	Altitude (m)	U	B	V	R	I	Reference
Rangapur	695	0.7-0.9	0.4-0.4	0.26-0.32			Kulkarni & Abhyankar 1978
IGO	1005		0.46	0.28			Das et al. 1999
Nainital	1951	0.57	0.28	0.17	0.11	0.07	Kumar et al. 2000
Devasthal	2450	0.49	0.32	0.21	0.13	0.08	Mohan et al. 1999
Kavalur	725	0.75	0.34	0.23			Singh et al. 1988
Leh	3500	0.50	0.28	0.17			Singh et al. 1988
KPNO	2120	0.622	0.281	0.162	0.119	0.075	Landolt & Uomoto 2007
La Silla	2400	0.424	0.271	0.164			Giraud et al. 2006
ALMA	5000	0.260	0.160	0.110			Giraud et al. 2006
Mauna Kea	4200	0.358	0.198	0.119	0.100	0.050	Mauna Kea 2005
Hanle	4467	0.36	0.21	0.12	0.09	0.05	This work

for sky brightness were acquired at various airmass ranges and therefore, the measured values of sky brightness need to be corrected for its dependence on zenith distance caused by the effects of airglow. To get the sky brightness at zenith, a correction (Δm) has been

Table 5. Yearly statistics of night sky brightness in mag/arcsec^2 at IAO. The errors given here are the standard deviation of the yearly measurements. In 2006, B and I bands have only one measurement each, and the errors are therefore not given.

Year	U	B	V	R	I
2003	22.19 ± 0.23	22.57 ± 0.09	21.21 ± 0.46	20.48 ± 0.48	18.79 ± 0.28
2004	22.33 ± 0.18	22.49 ± 0.26	21.30 ± 0.21	20.56 ± 0.38	18.90 ± 0.33
2005	22.10 ± 0.35	22.45 ± 0.22	21.32 ± 0.16	20.66 ± 0.29	18.92 ± 0.40
2006		22.30	21.21 ± 0.20	20.57 ± 0.19	18.58
2007	21.84 ± 0.22	22.14 ± 0.46	21.11 ± 0.20	20.34 ± 0.36	18.69 ± 0.20

Table 6. Comparison of night sky brightness in mag/arcsec^2 at various sites.

Site	U	B	V	R	I	Reference
La Silla	—	22.8	21.7	20.8	19.5	Mattila et al. 1996
Calar Alto	22.2	22.6	21.5	20.6	18.7	Leinert et al. 1995
La Palma	22.0	22.7	21.9	21.0	20.0	Benn & Ellison 1998
KPNO	—	22.9	21.9	—	—	Pilachowski et al. 1989
Mt. Graham	22.38	22.86	21.72	21.9	—	Taylor et al. 2004
CTIO	22.12	22.82	21.79	21.19	19.85	Krisciunas et al. 2007
Paranal	22.35	22.67	21.71	20.93	19.65	Patat 2008
SPM, Mexico	21.50	22.30	21.40	20.70	19.20	Tapia et al. 2007
Hanle	22.14	22.42	21.28	20.54	18.86	This work

added to the measured sky brightness following Patat (2003).

$$\Delta m = -2.5 log_{10} \left[(1-f) + fX \right] + k(X-1) \tag{11}$$

This assumes that a fraction(f) of the total sky brightness is generated by airglow, and the remaining (1-f) fraction is produced outside the atmosphere (thus including zodiacal light, faint stars and galaxies). To convert the measured sky brightness to zenith, the mean extinction values at IAO and $f = 0.6$ (Patat 2003) were used. Here X is the optical path length along a line of sight (not quite equivalent to the secant of zenith angle) and is given as (Patat 2003)

$$X = \left(1 - 0.96 sin^2 Z \right)^{-1/2} . \tag{12}$$

In order to estimate the night sky brightness during the dark moon period, the following criteria were applied while choosing the data from the IAO archives. They are (a) photometric conditions, (b) airmass ≤ 1.4, (c) galactic latitude $|b| > 10°$, (d) time distance from the closest twilight $\Delta t > 1$ hr and (e) no moon (fractional illumination of moon
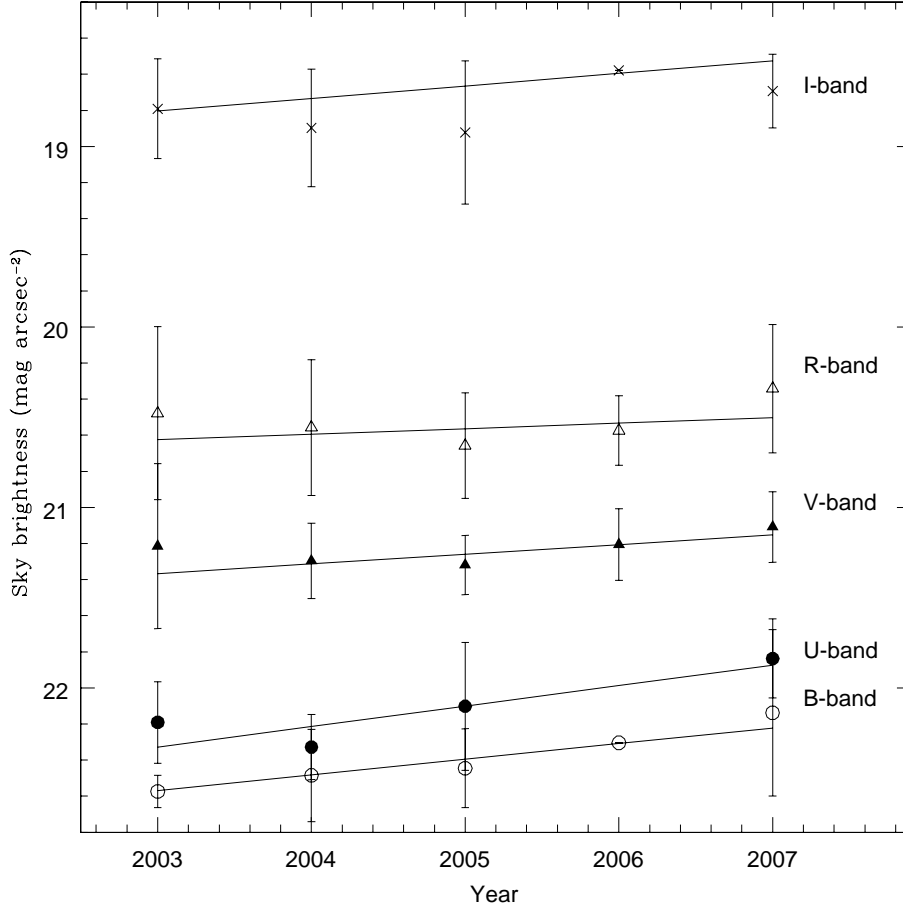
Figure 4. Yearly variation of night sky brightness in $UBVRI$ bands. The solid line is the unweighted linear least squares fit to the data. The error bars represent the scatter in the average values, the accuracy of individual measurements being much smaller. For the B and I bands in 2006 only one measurement is available in each band and hence the error bars are not plotted.

equal to zero or moon elevation $< -18°$). After applying these restrictions, we collected 210 frames, taken over 47 nights during 2003−2007. In this study, secondary standard stars (more than 6) were used in each frame and thus $E_* = E_{sky}$ in Eq. 9. It should be noted that the sky brightness at any line of sight towards the sky is not corrected for extinction following the method adopted in studies of sky brightness (Krisciunas et al. 2007).

The average moonless night sky brightness at the zenith at IAO are 22.14 ± 0.32 in U, 22.42 ± 0.30 in B, 21.28 ± 0.20 in V, 20.54 ± 0.37 in R and 18.86 ± 0.35 in I
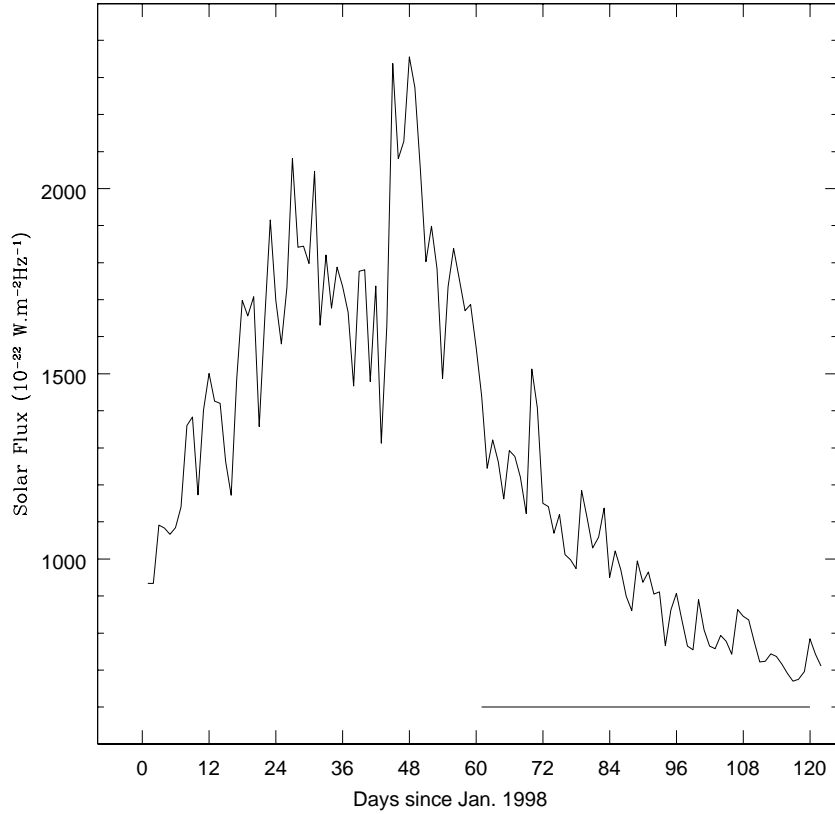
Figure 5. Average monthly solar flux at 10.7 cm since January 1998. The horizontal bar indicates the period (2003−2007) of sky brightness results presented here.

band. Their year wise statistics is given in Table 5 and their evolution over the year is shown in Fig. 4. The sky brightness evolution might not be significant and considering the errors, this might be consistent with no evolution. A comparison with other sites is given in Table 6. The sky brightness values at IAO listed in Table 6 are similar to those of other astronomical sites in $UBVR$ except I band. The sky at IAO in the I band is clearly brighter than the other astronomical sites listed in Table 6 with the exception of Calar Alto. This might be due to the hydorxy OH (Meinel) bands being stronger at IAO (see Section 5).

4.1 Variation of night sky brightness with solar activity

A possible correlation between sky brightness and solar activity was first pointed out by Rayleigh (1928) and Rayleigh & Jones (1935). It was later confirmed by several authors
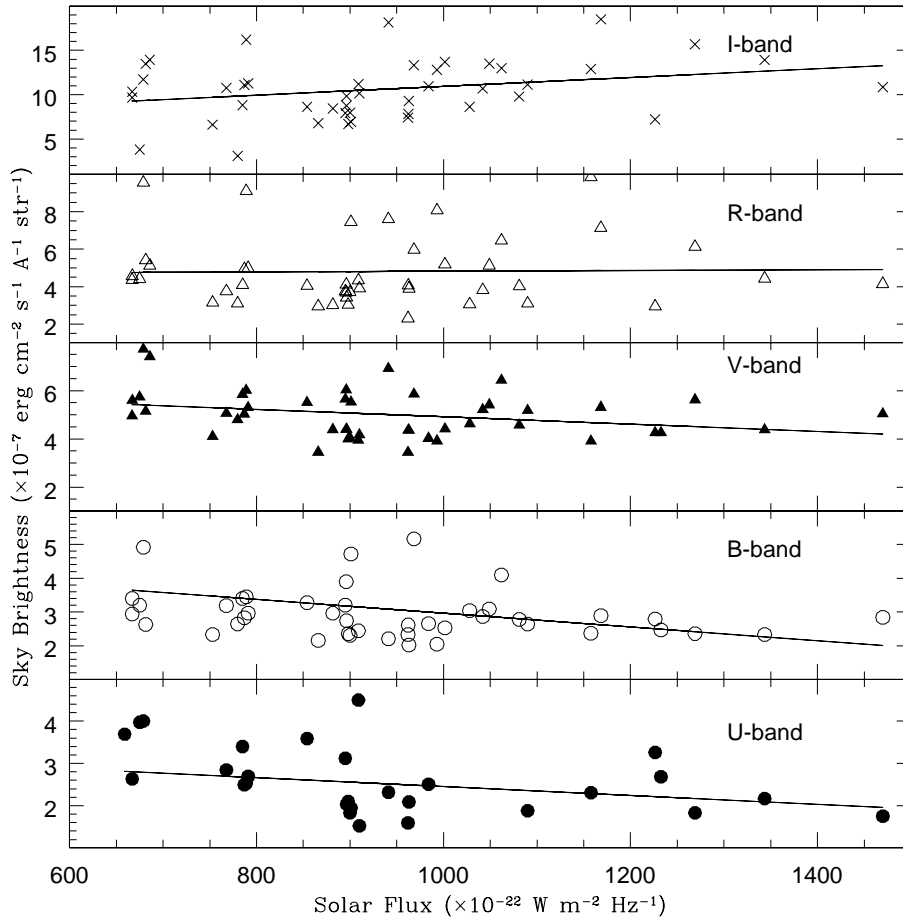
Figure 6. Variation of sky brightness with solar flux density at 10.7 cm. The solar flux density values are 10 days average prior to the date of measurement of sky brightness. The solid line is the linear least squares fit to the data.

(Walker 1988; Patat 2008; Krisciunas et al. 2007). The monthly averaged 2800 MHz solar flux[2] between Jan 1998−March 2008 is shown in Fig. 5. The data used in this work for sky brightness measurements covers the period 2003 to 2007 (shown as a horizontal bar in Fig. 5), and thus spans the declining phase of solar activity cycle−23. Our data can therefore be used to look for possible correlation between sky brightness and solar activity. For this, it might be more practical to use linear unit for sky brightness, contrary to the common astronomical practice of expressing sky brightness in magnitude per square arcsec. Following Patat (2003) the sky brightness in linear scale (expressed in erg s^{-1}
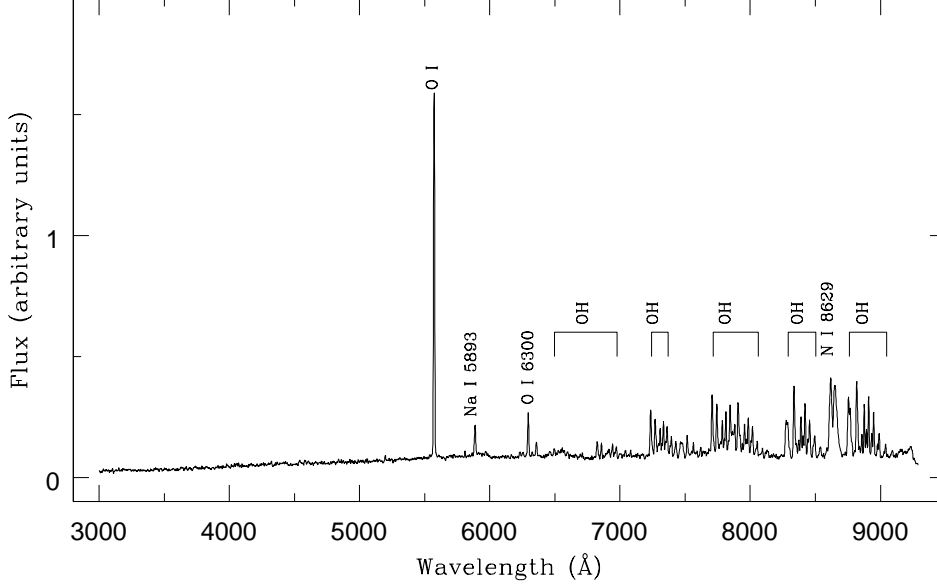
---

[2]http://www.ngdc.noaa.gov/stp/SOLAR/ftpsolarradio.html

Figure 7. Night sky spectrum at IAO, Hanle. Prominent sky lines are marked.

cm^{-2} $Å^{-1}$ sr^{-1}) is given as

$$B_\lambda = 10^{(-0.4(m_{sky,\lambda} - m_{0,\lambda} - 26.573))}. \tag{13}$$

Here, $m_{0,\lambda}$ is the magnitude zero point (Cox 2000), and $m_{sky,\lambda}$ is the measured sky brightness at zenith in mag arcsec^{-2}. Correlations have been looked for between measured sky brightness and average solar flux computed for 10 days prior to each sky brightness measurement. The results are shown in Fig. 6. A trend for a correlation is seen, though differently in various filters. To have a quantitative description of the correlation, a linear fit of the data to $m = m_0 + \gamma F_{sky}$ was done and the results of the fit are given in Table 7. From the low correlation coefficients, we point out that there is no correlation between sky brightness and solar activity, in this present data set. Similarly, no correlation between sky brightness and solar activity is found between the summer and winter months.

5.   Night sky spectrum

A typical night sky spectrum is shown in Fig. 7, and the data acquired for generating the spectrum is described in Section 2. The strong emission lines/bands clearly identified in the spectrum have been labelled with their corresponding atomic/molecular names, and a complete list of all the lines/bands identified in the spectra along with their respective strengths are listed in Table 8. The distinctive features seen in the night sky spectrum

Table 7. Linear regression analysis of night sky brightness v/s solar activity; $I_{\text{sky}}=a.\text{Flux}_{\text{star}}+b$.

Filter	a	b	R	npts
U	$3.51 \times 10^{-07} \pm 7.97 \times 10^{-08}$	$-1.05 \times 10^{-10} \pm 7.85 \times 10^{-11}$	-0.28	28
B	$5.01 \times 10^{-07} \pm 9.06 \times 10^{-08}$	$-2.04 \times 10^{-10} \pm 9.47 \times 10^{-11}$	-0.31	45
V	$6.44 \times 10^{-07} \pm 7.11 \times 10^{-08}$	$-1.52 \times 10^{-10} \pm 9.47 \times 10^{-11}$	-0.29	47
R	$4.64 \times 10^{-07} \pm 1.45 \times 10^{-07}$	$1.86 \times 10^{-11} \pm 1.53 \times 10^{-10}$	0.02	45
I	$5.93 \times 10^{-07} \pm 2.52 \times 10^{-07}$	$5.00 \times 10^{-10} \pm 2.66 \times 10^{-10}$	0.28	45

Table 8. Identified lines/bands in the night sky spectrum at IAO.

Wavelength (Å)	Species	E.Width (Å)	Wavelength (Å)	Species	E. Width (Å)
5577.3	[OI]	154.4	8062.4	OH	3.9
5891.6	Na I	17.3	8290.6	OH	56.3
6237.4	OH	4.2	8344.6	OH	30.9
6261.4	OH	4.2	8430.3	OH	18.2
6300.3	[OI]	23.1	8452.2	OH	6.8
6329.9	OH	1.7	8465.5	OH	18.2
6363.8	[OI]	8.5	8504.6	OH	13.4
6498.7	OH	4.7	8629.2	N I	50.9
6832.6	OH	10.1	8655.9	N I	72.3
6865.7	OH	10.9	8763.7	OH	45.0
6978.6	OH	4.4	8778.3	OH	25.0
7242.2	OH	30.3	8790.9	OH	9.0
7275.0	OH	20.8	8827.1	OH	37.1
7316.2	OH	7.3	8867.6	OH	8.6
7341.0	OH	14.8	8885.8	OH	17.6
7369.2	OH	10.5	8903.1	OH	7.7
7715.8	OH	26.6	8919.7	OH	20.9
7750.7	OH	20.5	8958.2	OH	15.8
7791.1	OH	8.0	8987.6	OH	5.5
7821.6	OH	10.3	9001.1	OH	13.4
7853.6	OH	9.6	9049.8	OH	6.7

are the OI lines (5577 and 6300 Å), OH rotational vibrational Meinel bands in the red region of the spectrum and lines due to Na and N.

6.   Conclusions

We have studied the nature of the night sky at IAO. The results are summarized below:

1. The measured average extinction coefficient at IAO during the period $2000-2008$ are 0.36 ± 0.07 in U, 0.21 ± 0.04 in B, 0.12 ± 0.04 in V, 0.09 ± 0.04 in R and 0.05 ± 0.03 in I. However, the average extinction during summer months is slightly larger than that of winter months. There is no clear evidence for a correlation between the measured extinction coefficient and the average night time wind speed.

2. The moonless night sky brightness at zenith are 22.14 ± 0.32 in U, 22.42 ± 0.30 in B, 21.28 ± 0.20 in V, 20.54 ± 0.37 in R and 18.86 ± 0.35 in I. Except for the I band, the sky brightness in other bands at IAO are similar to those of other dark sites in the world. The bright nature of the sky in I band at IAO, might be due to the presence of strong OH rotation vibrational Meinel bands in the red region of the optical spectrum. We find no dependence of the night sky brightness with 10.7 cm solar flux, probably due to insufficient data coverage during the solar cycle.

3. The moonless night sky spectrum covering the wavelength range 3000 to 9300 has been presented. Features from OI, OH, Na and N are seen in the spectra. Lines due to light pollution are not seen in the spectrum, and thus Hanle is free from any man-made light pollution.

We conclude that IAO has a night sky similar to the best sites in the world. In addition to the good skies, IAO also has a longitudinal advantage in covering the longitudinal gap between observatories in the West and the East. Hanle region could thus be a potential site for any future large Indian optical-infrared telescope(s).

7.   Acknowledgement

References

Benn, C.R., & Ellison, S.C., 1998, New Astronomy Review 42, 503
Bessel, M.S., 1990, PASP, 100, 496
Cox, A.N., 2000, *Allen's astrophysical quantities*, Springer
Das, H. K., Menon, S.M., Paranjpye, A., & Tandon, S.N., 1999, BASI, 27, 609
Giraud, E., Vasileiadis, G., Valvin, P., & Toledo, I., 2006, *astro-ph/0611262*
Guiterrex-Moreno, A., Moreno, H., & Cortes, G., 1982, PASP, 94, 722

Hayes, D.S., & Lantham, D. W., 1975, ApJ, 197, 593

Krisciunas, K., Semler, D.R., Richards, J., Schwarz, H., Suntzeff, N.B., Vera, S., & Sanhueza, P., 2007, PASP, 119, 687

Kriscuinas, K., 1997, PASP, 109, 1181

Kulkarni, A. G., & Abhyankar, K.D., 1978, BASI, 6, 43

Kumar, B., Sagar, R., Rautela, B.S., Srivastava, J. B., & Sirvastava, R.K., 2000, BASI, 28, 675

Landolt, A. U., 1992, AJ, 104, 340

Landolt, A. U., & Umoto, A. J., 2007, AJ, 133, 768

Leinert, Ch, Vaisanen, P., Mattila, K., & Lehtinen, K., 1995, A&AS, 112, 99

Mattila, K., Vaisanen, P., & Appen-Schnurr, G.F.O., 1996, A&AS, 119, 153

Mauna Kea 2005: http://www2.keck.hawaii.edu/inst/nirc/extrs.html

Mohan, V., Uddin, W., Sagar, R., & Gupta, S.K., 1999, BASI, 27, 601

Parihar, P.S., Sahu, D.K., Bhatt, B.C., Subramaniam, A., Anupama, G.C., & Prabhu, T.P., 2003, BASI, 31, 453

Patat, F., 2003, A&A, 400, 1183

Patat, F., 2008, A&A, 481, 575

Pilachowski, C. A., Africano, J. L., Goodrich, B. D., & Binkert, W. S., 1989, PASP, 101, 707

Rayleigh, L., 1928, Proc. Roy. Soc. London, Ser. A., 119, 11

Rayleigh, L., & Jones, H.S., 1935, Proc. Roy. Soc. London Ser. A., 151, 22

Rufener, F., 1986, A&A, 165, 275

Singh, J. et al. 1988, BASI, 16, 15

Stalin, C. S. , Shantikumar, N.S., Bhatt, B.C., Prabhu, T. P., Angchuk, D., Gorka, S., & Anupama, G. C., 2008, BASI *Submitted*

Sanchez, S.F., Aceituno, J., Thiele, U., Perez-Ramirez, D., & Alves, J., 2007, PASP, 119, 1186

Taylor, V.A., et al. 2004, PASP, 116, 762

Tapia, M., Cruz Gonzalez, I., & Avila, R., 2007, RevMexAA, 28 9

Walker, M.F., 1998, PASP, 100, 496